

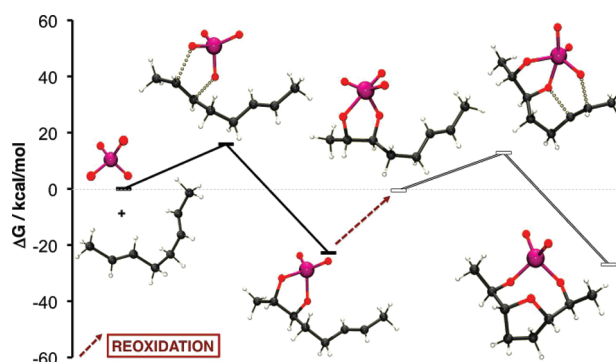
Stereoselective OsO₄-Catalyzed Oxidative Cyclization of 1,5-Dienes

Alexander Poethig and Thomas Strassner*

Professur für Physikalische Organische Chemie, Technische Universität Dresden, 01062 Dresden, Germany

thomas.strassner@chemie.tu-dresden.de

Received January 27, 2010



The mechanism of the oxidation of 1,5-dienes with osmium tetroxide was investigated by density functional theory calculations (B3LYP/6-311+G*). The observed products, 2,5-bis(hydroxymethyl)-tetrahydrofurans, are formed stereoselectively in a concerted reaction. Enantioselectivity could be induced by an enantioselective dihydroxylation followed by condensation of the 5,6-dihydroxyolefine with osmium tetroxide, while the diastereoselectivity is achieved by reaction of the 1,5-diene with osmium tetroxide and intermediate reoxidation of the osmium(VI) ester.

Introduction

Tetrahydrofuran derivatives are an important building block of biologically active molecules from both natural origin as well as from non-natural substances. Therefore, the motif of 2,5-disubstituted tetrahydrofurans can be found in a remarkable number of natural products of different classes, e.g., annonaceous acetogenins such as membrarollin or *cis*-sylvaticin, squalene-derived metabolites such as glabrescol, and polyether antibiotics such as monensin A

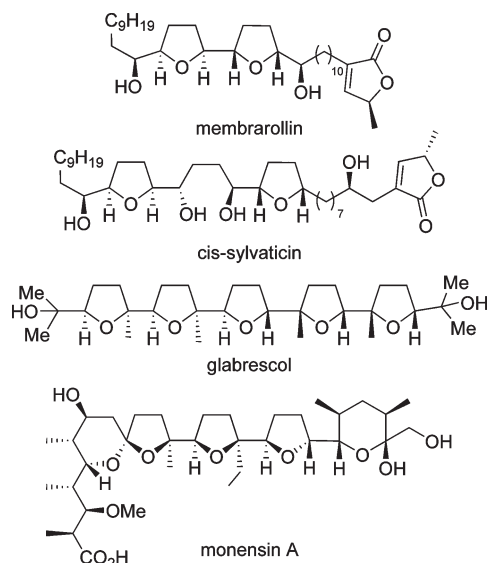
(Chart 1).^{1–6} These molecules potentially possess important biological activities, e.g., cytotoxic antitumor activity.^{7–12}

A convenient approach for the synthesis of those 2,5-disubstituted tetrahydrofuran units was developed throughout the last four decades. Oxidative cyclizations of dienes with metal-oxo compounds like permanganate, osmium tetroxide, ruthenium tetroxide, and perruthenate have been reported as early as 1965, when Klein and Rojahn used potassium permanganate to oxidize dienes.¹³ A more systematic investigation of these reactions has been carried out during the last ten years, but there still is a lack of understanding of the mechanisms and the stereochemical course of these transformations.¹⁴

After the initial observation by Klein and Rojahn, several groups studied the reaction with permanganate in greater detail, which led to miscellaneous suggestions for the mechanism.^{15–17}

- (1) Morris, C. L.; Hu, Y.; Head, G. D.; Brown, L. J.; Whittingham, W. G.; Brown, R. C. D. *J. Org. Chem.* **2009**, *74*, 981–988.
- (2) Bhunoo, R. A.; Hobbs, H.; Laine, D. I.; Light, M. E.; Brown, R. C. D. *Org. Biomol. Chem.* **2009**, *7*, 1017–1024.
- (3) Brown, L. J.; Spurr, I. B.; Kemp, S. C.; Camp, N. P.; Gibson, K. R.; Brown, R. C. D. *Org. Lett.* **2008**, *10*, 2489–2492.
- (4) Elliott, M. C. *J. Chem. Soc., Perkin Trans. 1* **2002**, 2301–2323.
- (5) Koert, U. *Synthesis* **1995**, 115–132.
- (6) Boivin, T. L. B. *Tetrahedron* **1987**, *43*, 3309–3362.
- (7) Alali, F. Q.; Liu, X.-X.; McLaughlin, J. L. *J. Nat. Prod.* **1999**, *62*, 504–540.
- (8) Bermejo, A.; Figadere, B.; Zafra-Polo, M.-C.; Barrachina, I.; Estornell, E.; Cortes, D. *Nat. Prod. Rep.* **2005**, *22*, 269–303.
- (9) Rupprecht, J. K.; Hui, Y. H.; McLaughlin, J. L. *J. Nat. Prod.* **1990**, *53*, 237–278.
- (10) Saez, J.; Sahpaz, S.; Villaescusa, L.; Hocquemiller, R.; Cave, A.; Cortes, D. *J. Nat. Prod.* **1993**, *56*, 351–356.

- (11) Zeng, L.; Ye, Q.; Oberlies, H.; Shi, G.; Gu, Z.-M.; He, K.; McLaughlin, J. L. *Nat. Prod. Rep.* **1996**, *13*, 275–306.
- (12) Zafra-Polo, M. C.; Figadere, B.; Gallardo, T.; Tormo, J. R.; Cortes, D. *Phytochemistry* **1998**, *48*, 1087–1117.
- (13) Klein, E.; Rojahn, W. *Tetrahedron* **1965**, *21*, 2353–2358.
- (14) Piccialli, V. *Synthesis* **2007**, 2585–2607.
- (15) Wolfe, S.; Ingold, C. F. *J. Am. Chem. Soc.* **1981**, *103*, 940–941.
- (16) Walba, D. M.; Wand, M. D.; Wilkes, M. C. *J. Am. Chem. Soc.* **1979**, *101*, 4396–4397.
- (17) Sable, H. Z.; Powell, K. A.; Katchian, H.; Niewoehner, C. B.; Kadlec, S. B. *Tetrahedron* **1970**, *26*, 1509–1524.

CHART 1. Examples for Tetrahydrofuran-Containing Natural Products


There is general agreement on the first reaction step, the formation of the manganese(V) ester, via a (3+2) cycloaddition.^{18,19} Labeling experiments with ¹⁸O-labeled water¹⁵ and previous results of our group, investigating the mechanism of the permanganate-promoted oxidative cyclization by DFT studies,²⁰ support the suggestion of an addition of a water molecule prior to the cyclization. A careful evaluation of the accessible potential energy hypersurfaces (PES) for the possible spin multiplicities singlet, triplet, and quintet even showed a two-state reactivity²¹ for the manganese, leading to a high-spin product. A two-state reactivity for permanganate had already been reported earlier.^{19,22}

Piccialli et al.²³ and Donohoe et al.²⁴ could perform analogous transformations using osmium tetroxide. Sharpless et al. observed the tetrahydrofuran derivatives as “abnormal oxidation” products when using ruthenium tetroxide.²⁵ The latter reaction could be applied to a wide range of 1,5-dienes²⁶ and scaled up under further-optimized conditions by Stark et al.^{27,28} Even an enantioselective version was established by Donohoe, who first introduced a defined stereochemistry by an asymmetric dihydroxylation followed by workup and isolation of the diol, which is then subjected to another equivalent of OsO₄.²⁹

For the oxidative cyclization with OsO₄ a similar reaction pathway as in the case of permanganate could be suggested (Scheme 1). The (2+2) reaction pathway was ruled out, also for osmium tetroxide, based on thorough mechanistic investigations by density functional theory calculations.^{30–34} The first reaction step again would be a (3+2) cycloaddition, leading to an osmium(VI) ester. Afterwards, the reaction could theoretically proceed to an osmium(IV) ester, followed by reoxidation to Os(VIII) (Scheme 1, path A).

But there is a significant difference: the permanganate is used stoichiometrically whereas the osmium reaction is catalytic. Hence, there are more possibilities to consider for the nature of the oxidizing metal–oxo species. Thus, the intermediate osmium(VI) ester could be reoxidized to an Os(VIII) species before reacting with the second double bond (Scheme 1, path B). Following this pathway the oxidation state of osmium would just change between Os(VIII) and Os(VI), which has been observed before for double bond oxidations with osmium.³⁵

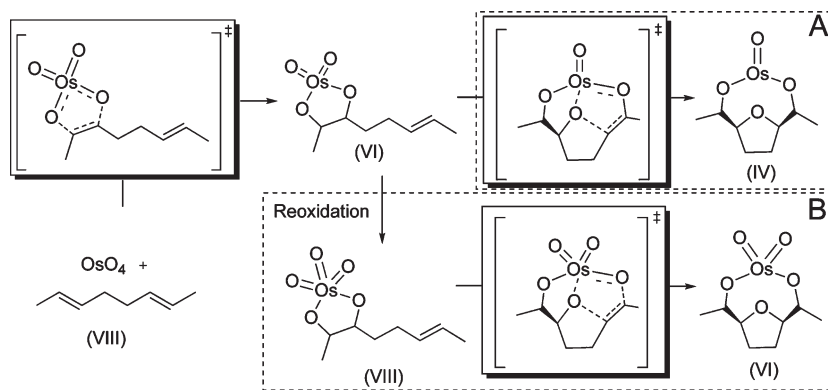
As we previously did for permanganate, we investigated the reaction mechanism for the different possible potential energy hypersurfaces, wondering whether osmium shows a similar behavior. The addition of a water molecule was also considered, as it is known from the so-called “ligand accelerating effect” in the case of dihydroxylation by OsO₄ that osmium tetroxide can add ligands to its coordination sphere.³⁶ Since we found a completely different behavior for osmium compared to permanganate, we refer to prior results in this paper to directly illustrate the differences and discuss possible reasons.

Computational Details

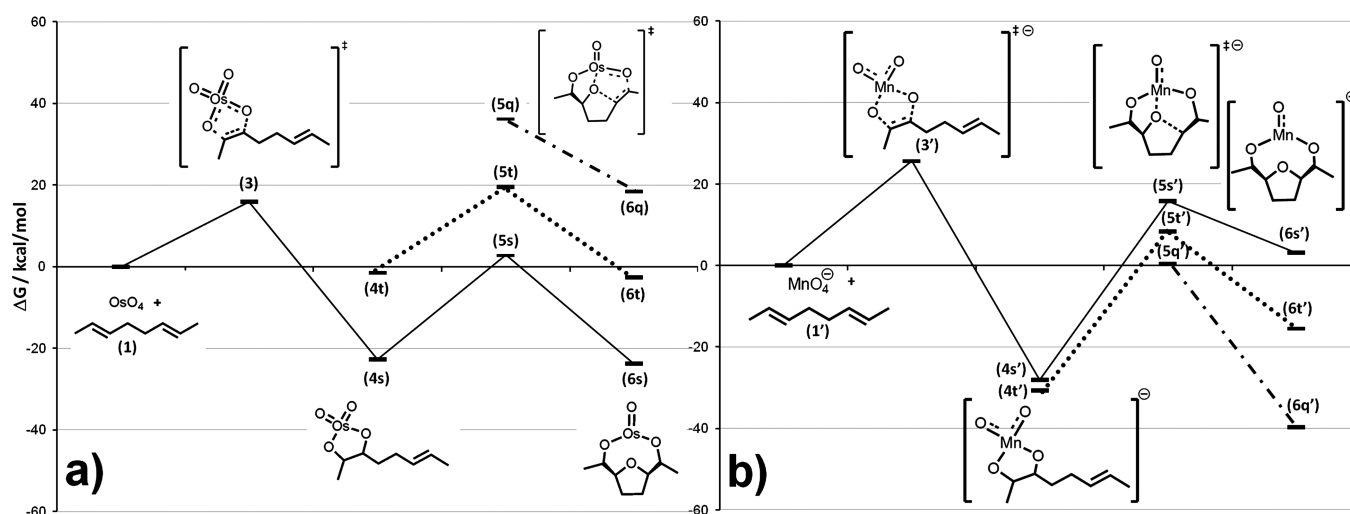
All calculations were performed with GAUSSIAN-03,³⁷ using the density functional/Hartree–Fock hybrid model Becke3LYP^{38–41} and the split valence triple- ζ (TZ) basis set 6-311+G(d)^{42–49} for

(18) Houk, K. N.; Strassner, T. *J. Org. Chem.* **1999**, *64*, 800–802.
 (19) Strassner, T.; Busold, M. *J. Org. Chem.* **2001**, *66*, 672–676.
 (20) Poethig, A.; Strassner, T. *Collect. Czech. Chem. Commun.* **2007**, *72*, 715–727.
 (21) Schroeder, D.; Shaik, S.; Schwarz, H. *Acc. Chem. Res.* **2000**, *33*, 139–145.
 (22) Strassner, T.; Busold, M. *J. Phys. Chem.* **2004**, *108*, 4455–4458.
 (23) De Champdore, M.; Lasalvia, M.; Piccialli, V. *Tetrahedron Lett.* **1998**, *39*, 9781–9784.
 (24) Donohoe, T. J.; Winter, J. J. G.; Helliwell, M.; Stemp, G. *Tetrahedron Lett.* **2001**, *42*, 971–974.
 (25) Carlsen, P. H. J.; Katsuki, T.; Martin, V. S.; Sharpless, K. B. *J. Org. Chem.* **1981**, *46*, 3936–3938.
 (26) Piccialli, V.; Cavallo, N. *Tetrahedron Lett.* **2001**, *42*, 4695–4699.
 (27) Goehler, S.; Roth, S.; Cheng, H.; Goeksel, H.; Rupp, A.; Haustedt, L. O.; Stark, C. B. W. *Synthesis* **2007**, 2751–2754.
 (28) Roth, S.; Goehler, S.; Cheng, H.; Stark, C. B. W. *Eur. J. Org. Chem.* **2005**, 4109–4118.
 (29) Donohoe, T. J.; Butterworth, S. *Angew. Chem., Int. Ed.* **2005**, *44*, 4766–4768.

(30) Deubel, D. V.; Frenking, G. *Acc. Chem. Res.* **2003**, *36*, 645–651.
 (31) DeMonte, A. J.; Haller, J.; Houk, K. N.; Sharpless, K. B.; Singleton, D. A.; Strassner, T.; Thomas, A. A. *J. Am. Chem. Soc.* **1997**, *119*, 9907–9908.
 (32) Pidun, U.; Boehme, C.; Frenking, G. *Angew. Chem., Int. Ed.* **1997**, *35*, 2817–2820.
 (33) Torrent, M.; Deng, L.; Duran, M.; Sola, M.; Ziegler, T. *Organometallics* **1997**, *16*, 13–19.
 (34) Dapprich, S.; Ujaque, G.; Maseras, F.; Lledos, A.; Musaev, D. G.; Morokuma, K. *J. Am. Chem. Soc.* **1996**, *118*, 11660–11661.
 (35) Kolb, H. C.; VanNieuwenhze, M. S.; Sharpless, K. B. *Chem. Rev.* **1994**, *94*, 2483–2547.
 (36) Jacobsen, E. N.; Marko, I.; Mungall, W. S.; Schroeder, G.; Sharpless, K. B. *J. Am. Chem. Soc.* **1988**, *110*, 1968–1970.
 (37) Frisch, M. J. et al.; *Gaussian 03*, Revision C.02; Gaussian, Inc., Wallingford, CT, 2004.
 (38) Becke, A. D. *J. Chem. Phys.* **1993**, *98*, 5648–5652.
 (39) Lee, C. Y., W.; Parr, R. G. *Phys. Rev. B: Condens. Matter* **1988**, *37*, 785–789.
 (40) Stephens, P. J.; Devlin, F. J.; Chabalowski, C. F.; Frisch, M. J. *J. Phys. Chem.* **1994**, *98*, 11623–11627.
 (41) Vosko, S. H.; Wilk, L.; Nusair, M. *Can. J. Phys.* **1980**, *58*, 1200–1211.
 (42) Binning, R. C., Jr.; Curtiss, L. A. *J. Comput. Chem.* **1990**, *11*, 1206–1216.
 (43) Clark, T.; Chandrasekhar, J.; Spitznagel, G. W.; Schleyer, P. v. R. *J. Comput. Chem.* **1983**, *4*, 294–301.
 (44) Frisch, M. J.; Pople, J. A.; Binkley, J. S. *J. Chem. Phys.* **1984**, *80*, 3265–3269.
 (45) Hay, P. J. *J. Chem. Phys.* **1977**, *66*, 4377–4384.
 (46) Krishnan, R.; Binkley, J. S.; Seeger, R.; Pople, J. A. *J. Chem. Phys.* **1980**, *72*, 650–654.
 (47) McGrath, M. P.; Radom, L. *J. Chem. Phys.* **1991**, *94*, 511–516.
 (48) Raghavachari, K.; Trucks, G. W. *J. Chem. Phys.* **1989**, *91*, 2457–2460.
 (49) Wachters, A. J. H. *J. Chem. Phys.* **1970**, *52*, 1033–1036.

SCHEME 1. Possible Reaction Pathways for the Osmium-Catalyzed Cyclization^a

^aPath A: Os(VIII) → Os(VI) → Os(IV). Path B: Os(VIII) → Os(VI) → Os(VIII) → Os(VI).

SCHEME 2. Reaction Path^a

^aPanel a: Os(VIII) → Os(VI) → Os(IV). The solid line (—) marks the singlet potential energy surface (PES), the dotted line (···) the triplet PES, and the semidotted line (•—•) the quintet PES. (b) Reaction path for permanganate-promoted cyclization.²⁰

C, H, and O. For Os, a Hay–Wadt VDZ ($n+1$) ECP was used.⁵⁰ Though B3LYP may overestimate the energies of states with higher multiplicities, it is in general an advisable functional and overall works well, especially for transition metals.^{51–53}

No symmetry or internal coordinate constraints were applied during optimizations. All reported intermediates were verified as being true minima by the absence of negative eigenvalues in the vibrational frequency analysis. Transition state structures were located by using the Berny algorithm⁵⁴ until the Hessian matrix had only one imaginary eigenvalue. The identities of all transition states were checked by animating the negative eigen-

vector coordinate with MOLDEN⁵⁵ and GaussView,⁵⁶ for selected transition states by IRC calculations.⁵⁷

The results shown are given for the different potential energy hypersurfaces (PES) as referred to in the text. Approximate free energies (ΔG) and enthalpies (ΔH) were obtained through thermochemical analysis of frequency calculations, using the thermal correction to Gibbs free energy as reported by GAUSSIAN-03. This takes into account zero-point effects, thermal enthalpy corrections, and entropy. All energies reported in this paper, unless otherwise noted, are free energies or enthalpies at 298 K, using unscaled frequencies.

Results and Discussion

The simplest mechanism possible for the oxidation of octa-2,6-diene **1** was first examined on the singlet potential energy surface (PES) as shown in Scheme 2. The first step of the reaction on the singlet surface, leading to the osmium(VI) ester **4s** via the transition state **3**, is exergonic ($\Delta G = -22.8$ kcal/mol) and has an activation barrier of 15.9 kcal/mol (Table 1). The following reaction (**4s** → **6s**) proceeds through transition state **5s** ($\Delta G^\ddagger = 2.9$ kcal/mol) with an activation barrier of 25.7 kcal/mol. **5s** (like transition state **3**) was found

(50) Hay, P. J.; Wadt, W. R. *J. Chem. Phys.* **1985**, *82*, 299–310.

(51) Reiher, M.; Salomon, O.; Hess, B. A. *Theor. Chem. Acc.* **2001**, *107*, 48–55.

(52) Salomon, O.; Reiher, M.; Hess, B. A. *J. Chem. Phys.* **2002**, *117*, 4729–4737.

(53) Strassner, T.; Taige, M. A. *J. Chem. Theory Comput.* **2005**, *1*, 848–855.

(54) Schlegel, H. B. *J. Comput. Chem.* **1982**, *3*, 214–218.

(55) Schaftenaar, G.; Noordik, J. H. *J. Comput.-Aided Mol. Design* **2000**, *14*, 123–134.

(56) Dennington, R. I.; Keith, T.; Millam, J. M.; Eppinnett, W.; Hovell, W. L.; Gilliland, R. *GaussView, 3.09*; Gaussian Inc.: Wallingford, CT, 2003.

(57) Fukui, K. *Acc. Chem. Res.* **1981**, *14*, 363–368.

TABLE 1. Thermodynamic Data of All Calculated Structures and Stabilization Effects $\Delta\Delta G$ Due to the Addition of a Water Molecule^a

structure	without water			with water			stabilization $\Delta\Delta G$ (kcal/mol)
	ΔH (kcal/mol)	ΔG (kcal/mol)	ΔS (cal/(K·mol))	ΔH (kcal/mol)	ΔG (kcal/mol)	ΔS (cal/(K·mol))	
1 + 2	0.0	0.0	0.0				
3	3.4	15.9	-41.8				
4s	-36.6	-22.8	-46.5	-52.7	-27.0	-86.2	-4.2
4t	-14.9	-1.6	-44.4	-31.4	-7.0	-82.0	-5.4
5s	-15.3	2.9	-61.0	-25.6	3.5	-97.7	0.6
5t	2.4	19.5	-57.6	-10.2	18.4	-96.0	-1.1
5q	19.6	36.2	-55.9	4.1	31.3	-91.2	-4.9
6s	-42.1	-23.8	-61.7	-50.0	-21.4	-96.2	2.4
6t	-19.3	-2.6	-56.1	-42.4	-14.7	-92.9	-12.1
6q	2.2	18.4	-54.2	-38.4	-11.4	-90.7	-29.8
4s ^{ox}	-42.4	-28.7	-46.0	-30.0	-5.1	-83.6	-23.6
5s ^{ox}	-33.0	-15.6	-58.2	-23.9	+4.9	-96.4	-20.5
6s ^{ox}	-72.0	-54.6	-58.6	-96.6	-67.2	-98.7	12.6

^aKey: s, singlet ; t, triplet ; q, quintet structures. The bold values show the free energies of the preferred reaction pathway.

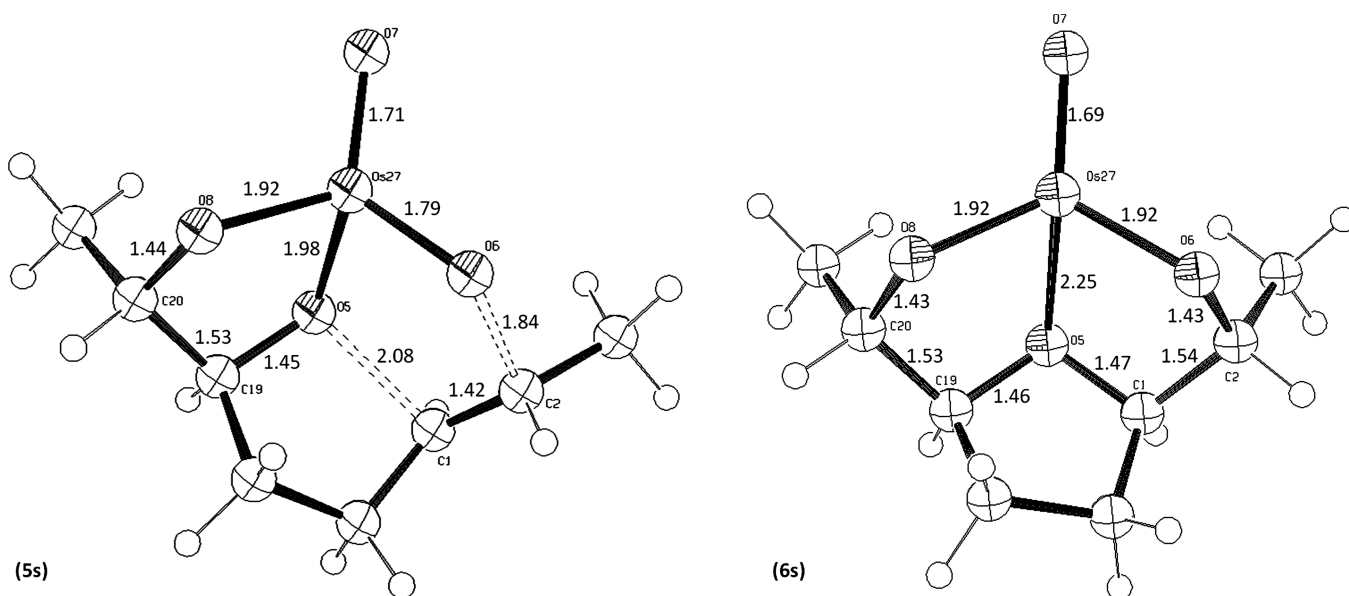


FIGURE 1. Transition state 5s (Os(VI) \rightarrow Os(IV)) and complex 6s with selected bond lengths (in Å).

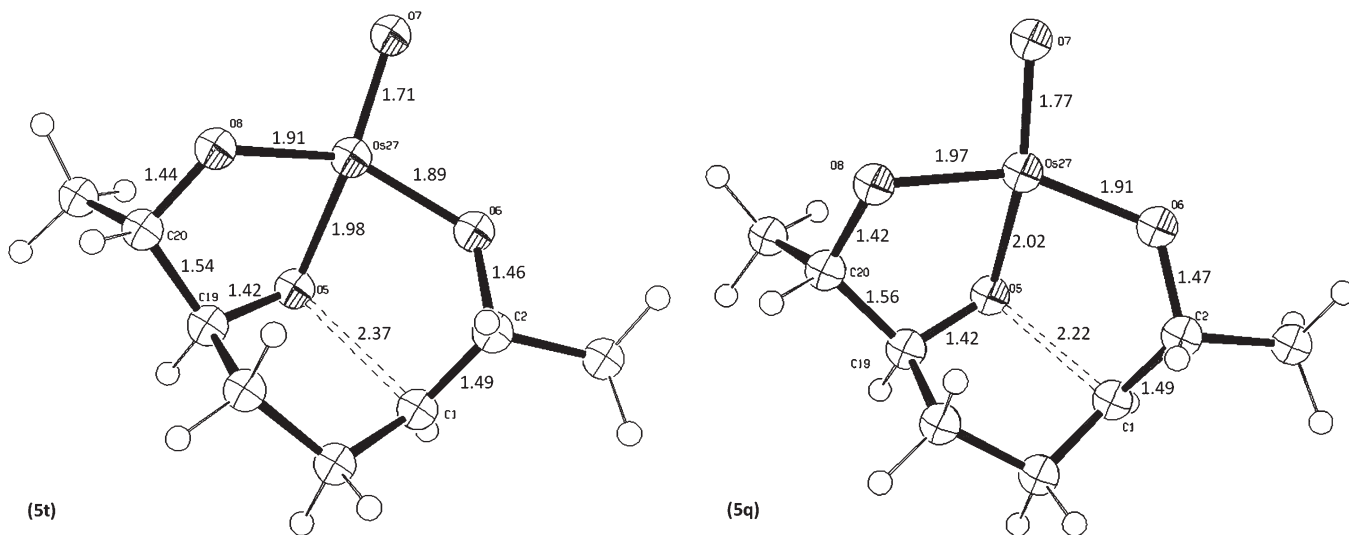
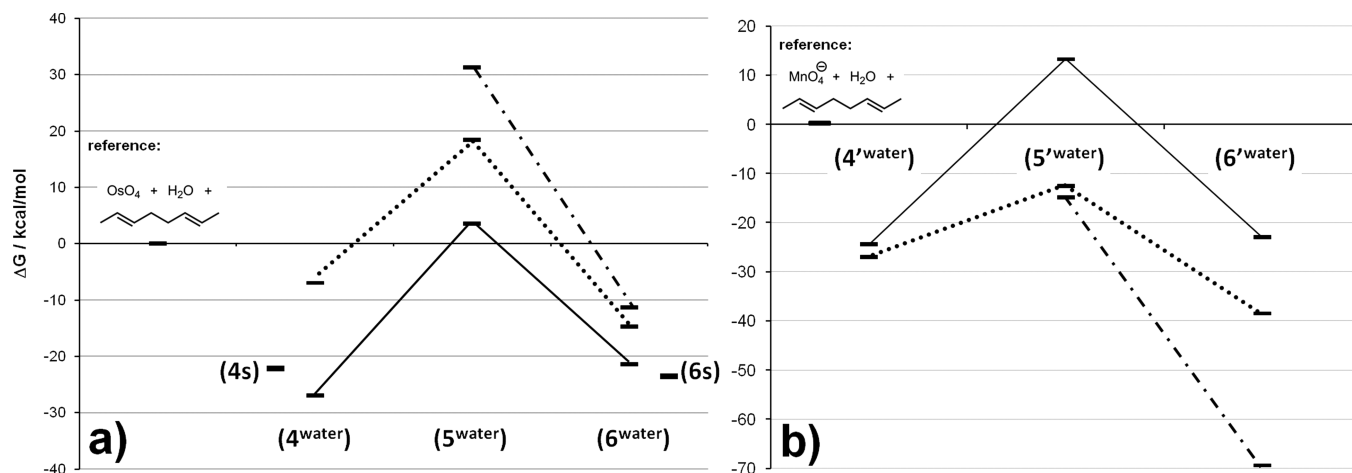
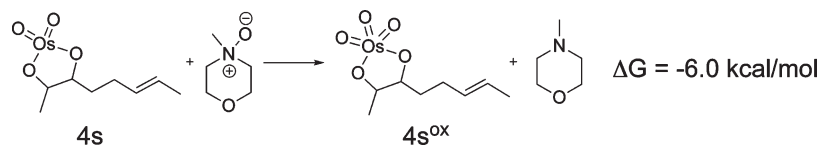
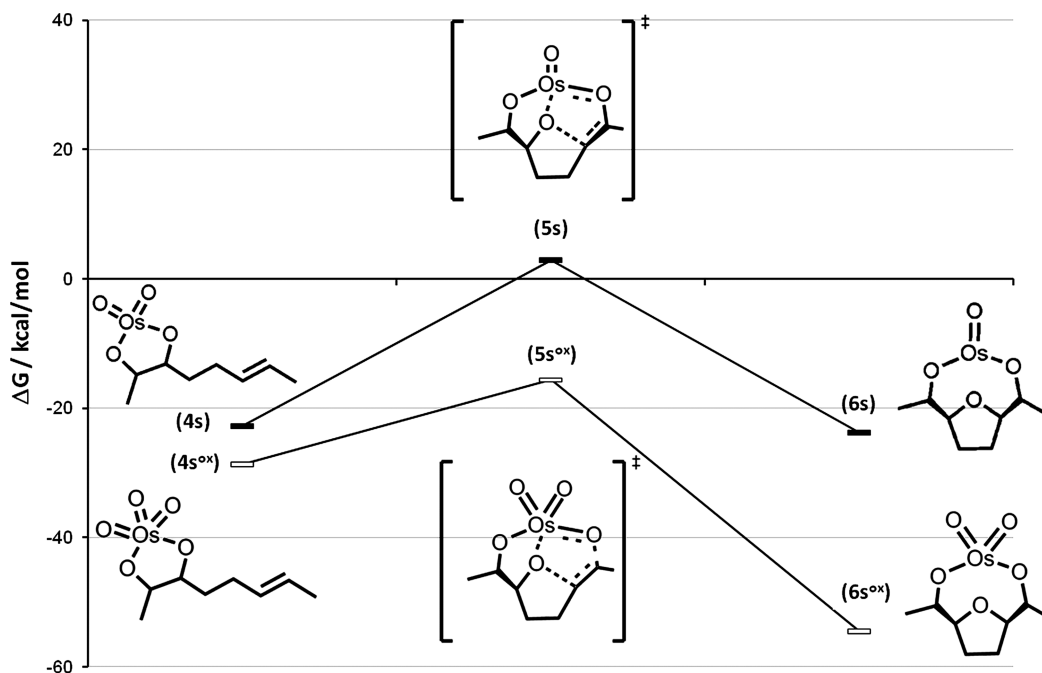


FIGURE 2. Transition states 5t and 5q (Os(VI) \rightarrow Os(IV)) with selected bond lengths (in Å).

SCHEME 3. Cyclization Step after Water Addition^a

^aPanel a: $\text{Os(VI)} \rightarrow \text{Os(IV)}$. The solid line (—) marks the singlet potential energy surface (PES), the dotted line (···) the triplet PES, and the semidotted line (•-•) the quintet PES. Panel b: Reaction path for permanganate-promoted cyclization.²⁰ Energies are referenced to the individual starting materials.

SCHEME 4. Reoxidation of the Intermediate from Os(VI) to Os(VIII)

SCHEME 5. Cyclization Step after Reoxidation^a

^aReaction path without (**4s** \rightarrow **6s**) and with (**4s^{ox}** \rightarrow **6s^{ox}**) prior reoxidation of the Os(VI) species on the singlet PES. Energies are referenced to the individual starting materials.

to follow a (3+2) cycloaddition (Figure 1). The almost thermoneutral cyclization step finally leads to the product **6s** (Figure 1), which is only 1 kcal/mol lower in energy compared to **4s**.

We also checked whether the osmium(VI) intermediate **4** can access different potential energy hypersurfaces, but found the osmium(VI) ester **4t** (on the triplet surface) to be significantly higher in energy by 21.2 kcal/mol than the

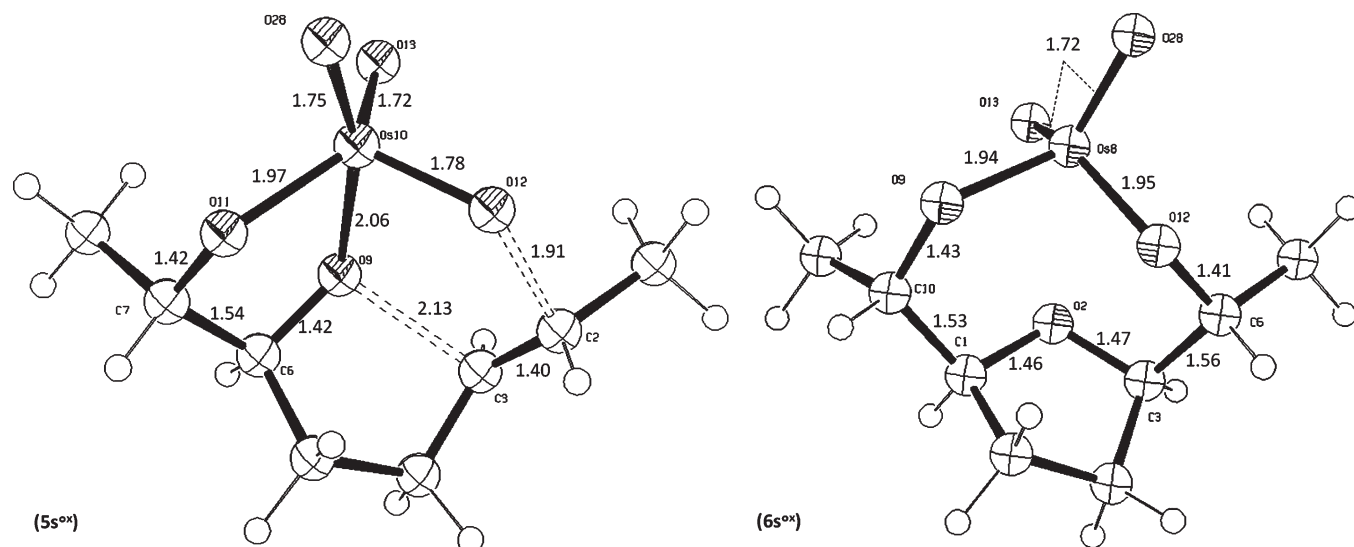


FIGURE 3. Transition state $5s^{ox}$ (Os(VIII) \rightarrow Os(VI)) and product $6s^{ox}$ (Os(VI)) with selected bond lengths (in Å).

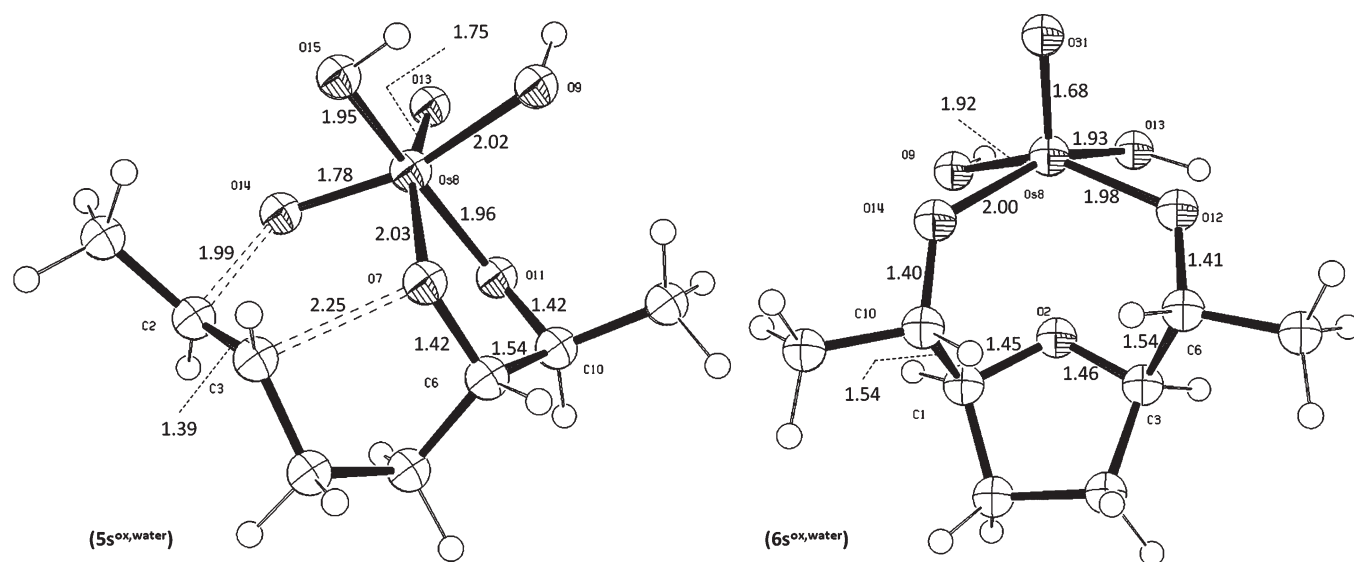


FIGURE 4. Transition state $5s^{ox,water}$ (Os(VIII) \rightarrow Os(VI)) and product $6s^{ox,water}$ (Os(VI)) with selected bond lengths (in Å).

corresponding intermediate **4s** in the singlet state. Comparison of the geometries and Gibbs free energies with the permanganate reaction (Scheme 2b) for the intermediates **4'** shows a significant difference.²⁰ While in the permanganate case the energy difference between singlet and triplet state is small enough to allow a change of the hypersurface, this is not the case for **4s** and **4t**.

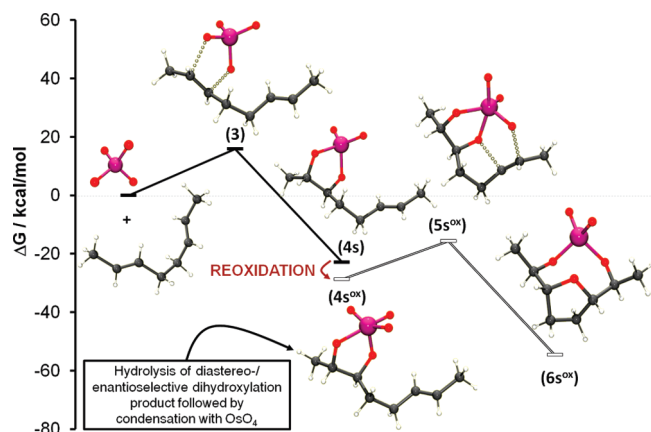
For osmium we also found the transition states and products with higher multiplicities to be significantly higher in energy compared to those on the singlet PES. With $\Delta G^\ddagger = 19.5$ (**5t**) and 36.2 kcal/mol (**5q**) the transition state on the triplet PES is 16.6 kcal/mol and that on the quintet PES 33.3 kcal/mol higher in energy compared to **5s**. The results for the products **6** differ by about 21 kcal/mol for each of the hypersurfaces (**6s**: $\Delta G = -23.8$ kcal/mol; **6t**: $\Delta G = -2.6$ kcal/mol; **6q**: $\Delta G = 18.4$ kcal/mol).

In contrast to **5s**, our previous calculations for the transition states of the permanganate-promoted oxidative cycli-

zation led to structures with the distal oxygen (Figure 2, O6) already being attached to the second double bond while the central oxygen is closing the THF ring.²⁰ In the OsO₄-catalyzed reaction we got similar geometries for the transition states **5t** and **5q** (Figure 2), although they are too high in energy to be the product-forming transition states.

As expected, all Os–O bonds elongate with increasing multiplicity because of the higher number of unpaired electrons and the resulting higher single bond character. Therefore, the asynchronicity of the bond formation increases compared to that of the more concerted reaction in the case of **5s**, which is also true for the product-forming transition states of the permanganate high-spin PES.²⁰

Addition of Water. In the case of osmium, the addition of a water molecule did not show a comparable stabilization in energy as it did with permanganate regarding the ongoing reaction (Scheme 3a). Although the intermediate **4s^{water}**, formed by addition of the water molecule to **4s**, is

SCHEME 6. Suggested Overall Reaction Pathway^a

^aSinglet hypersurface with reoxidation of the intermediate Os(VI) ester (Os(VIII) → Os(VI) → Os(VIII) → Os(VI)). Enantioselective cyclization requires the reaction of OsO₄ with the product of an enantioselective dihydroxylation forming intermediate 4s^{ox}.

4.2 kcal/mol lower in energy, the overall reaction is endergonic. The slightly exergonic reaction step (4s → 6s) would be changed into an endergonic step (4s^{water} → 6s^{water}) with an activation barrier of 30.5 kcal/mol (Table 1: 4s^{water}, 5s^{water}, 6s^{water}). This is a first significant difference to the permanganate promoted reaction, for which the addition of a water molecule after the cycloaddition to the first double bond was shown to play a crucial role, since it lowered the activation barriers as well as the absolute Gibbs free energies for the product complexes on the PES for every multiplicity, but to a greater extent than for the higher multiplicities (Scheme 3b).²⁰

For the osmium-catalyzed reaction the calculated free energies on triplet and quintet PES are always higher compared to that on the singlet surface (Scheme 3a). Whereas for the permanganate reaction the addition of water has a dramatic effect on the reaction profile, we can rule out a similar addition of water to the osmium(VI) species.

Reoxidation of Os(VI) to Os(VIII). The catalytic nature of the cyclization reaction with use of OsO₄ opens up additional possible reaction pathways. A reoxidation of the intermediate osmium(VI) ester 4s to the osmium(VIII) ester 4s^{ox} with, e.g., *N*-methylmorpholine *N*-oxide (NMO) as a co-oxidant is conceivable and was investigated by calculating the thermochemistry of this transformation, using the lowest energy conformations of NMO and NM. (Scheme 4).

Starting from the reoxidized Os(VIII) intermediate 4s^{ox} (Scheme 2, pathway B), we also found the oxidation of the second double bond to be energetically favored compared to that starting from the osmium(VI) species (Scheme 5).

With 13.1 kcal/mol the cyclization step (4s^{ox} → 6s^{ox}) has a lower activation barrier compared to the 25.7 kcal/mol without reoxidation (4s → 6s). The product-forming transition state 5s^{ox} with ΔG[‡] = -15.6 kcal/mol is 18.5 kcal/mol lower in energy than the corresponding transition state 5s (Scheme 1, pathway A) without reoxidation. The product

6s^{ox} (Figure 3) shows a larger stabilization of 30.8 kcal/mol compared to its corresponding Os(IV) compound (6s). A possible reason for this additional stabilization can be found in the coordination geometry since due to the additional oxygen atom at 6s^{ox} the oxygen atoms are able to form an only slightly distorted tetrahedron around the osmium. In the case of 6s the coordination of the oxygen in the THF-ring leads to a more distorted geometry. This also explains the shorter Os–O(THF) bond (2.25 Å) compared to that of 6s^{ox} (2.50 Å). The cyclization step after reoxidation is exergonic by -25.9 kcal/mol and therefore also thermodynamically favored in comparison to the cyclization without reoxidation.

We also evaluated whether a possible addition of a water molecule to the oxidized species leads to a stabilizing effect. The transition state 5s^{ox,water} (Figure 4, left) could be found to be significantly higher in energy than 5s^{ox}, leading to a higher activation barrier for the cyclization step, which energetically disfavors this reaction pathway.

In contrast 6s^{ox,water} shows a stabilization of 12.6 kcal/mol due to the addition of the water molecule but we can rule out that this addition of water has an important effect on the formation of the tetrahydrofuran ring, since the stabilization takes place after the ring closure.

Conclusion

We investigated the osmium tetroxide-catalyzed oxidative cyclization of 1,5-dienes by performing density functional theory calculations (B3LYP/6-311+G*). We found the reaction to proceed on the singlet hypersurface via the oxidation states Os(VIII) → Os(VI) → Os(VIII) → Os(VI) including an intermediate reoxidation of the osmium(VI) to osmium(VIII) after the first (3+2) cycloaddition, leading to a lower activation energy of the following cyclization step (Scheme 6).

Contrary to the similar transformation by permanganate, neither a high spin state could be found to be favored, nor the addition of a water molecule led to a significant stabilization. The barrier for the first reaction step was shown to be significantly lower compared to that for permanganate, which might be a reason for the advantage of using osmium tetroxide in some reactions, where the transformation with permanganate fails.¹⁴ The reaction with osmium tetroxide is less exergonic since osmium is already reoxidized after the first reaction step, dividing the process in two separate steps with only -22.8 and -25.9 kcal/mol, i.e., the overall reaction does not end up in a thermodynamic sink, which is crucial for a catalytic reaction.

Acknowledgment. A.P. thanks the Fonds der Chemischen Industrie for financial support and the center of highperformance computing (ZIH) of the TU Dresden for providing the computing time.

Supporting Information Available: Complete ref 37, Cartesian coordinates, and results of the frequency calculations of the optimized structures. This material is available free of charge via the Internet at <http://pubs.acs.org>.